

Discriminative Perception via Anchored Description for Reasoning Segmentation

Tao Yang*, Qing Zhou*, Yanliang Li, Qi Wang[†]
Northwestern Polytechnical University

{taoytao, mrazhou, yanliangli}@mail.nwpu.edu.cn, crabwq@gmail.com

Abstract

Reasoning segmentation increasingly employs reinforcement learning to generate explanatory reasoning chains that guide Multimodal Large Language Models. While these geometric rewards are primarily confined to guiding the final localization, they are incapable of discriminating whether the reasoning process remains anchored on the referred region or strays into irrelevant context. Lacking this discriminative guidance, the model’s reasoning often devolves into unfocused and verbose chains that ultimately fail to disambiguate and perceive the target in complex scenes. This suggests a need to complement the RL objective with Discriminative Perception, an ability to actively distinguish a target from its context. To realize this, we propose DPAD to compel the model to generate a descriptive caption of the referred object, which is then used to explicitly discriminate by contrasting the caption’s semantic relevance to the referred object against the wider context. By optimizing for this discriminative capability, the model is forced to focus on the unique attributes of the target, leading to a more converged and efficient reasoning chain. The descriptive caption also serves as an interpretability rationale that aligns with the segmentation. Experiments on the benchmarks confirm the validity of our approach, delivering substantial performance gains, with the cIoU on ReasonSeg increasing by 3.09% and the reasoning chain length decreasing by approximately 42%. Code is available at <https://github.com/mrazhou/DPAD>.

1. Introduction

Reasoning segmentation (RS) [12, 26, 28] challenges models to generate precise pixel-level masks by interpreting nuanced, context-dependent language queries. The task requires the model to perform inference, deciphering implicit relational and attributive cues within a query to isolate the target within a complex visual scene. The advent of Multimodal Large Language Models (MLLMs) has

*Equal contribution.

[†]Corresponding author.



Figure 1. Comparison between Seg-Zero’s unfocused reasoning (green), which leads to lower performance, and DPAD’s focused reasoning (blue), which is guided by Discriminative Perception to achieve substantial improvements.

been pivotal in addressing this challenge [17, 23], leading to architectures that bridge their powerful reasoning capabilities with specialized segmentation modules to achieve language-guided, pixel-level understanding.

Early architectures like the pioneering LISA [11] relied on Supervised Fine-Tuning (SFT). The limited out-of-distribution (OOD) generalization of this approach [12, 17], however, catalyzed a paradigm shift towards Reinforcement Learning (RL) to cultivate more generalizable reasoning [3, 8, 23]. Within this shift, Group-Relative Policy Optimization (GRPO) [7] has emerged as a compelling choice, demonstrating substantial advantages for fine-tuning models on task-specific rewards [18, 25, 27, 33]. This RL approach facilitated emergent reasoning, where models autonomously generate Chains-of-Thought, directly improv-

ing OOD adaptability in visual tasks. Drawing on this emergent reasoning, several works [17, 23, 27, 29] in RS have demonstrated that a pure RL strategy can generate reasoning chains to navigate cluttered visual contexts, achieving substantial zero-shot performance improvements on challenging benchmarks such as ReasonSeg.

Despite their success, these RL-driven paradigms are fundamentally limited by a core learning signal that relies on reward functions based on geometric metrics like IoU and L1 distance [9]. While these geometric metrics are primarily confined to guiding the final localization, they offer only indirect or insufficient incentives for the intermediate reasoning process. Indeed, they are incapable of discriminating whether the reasoning process remains anchored on the referred region or strays into irrelevant context. Lacking this discriminative guidance, the model’s reasoning can often devolve into chains that are divergent, unanchored, and verbose. This deficiency is particularly detrimental when effective disambiguation and discerning perception are required, as a divergent reasoning chain inevitably incorporates irrelevant contextual distractors, polluting the semantic cues the model relies on [1, 19, 24]. As a result, the model struggles to isolate the true target from a complex scene, as shown in Figure 1. To address this critical gap, we propose a complementation in the learning objective for RS itself—moving beyond mere geometric accuracy to actively cultivate the model’s ability to distinguish the target from its context, a capability termed Discriminative Perception.

We realize Discriminative Perception through our method, DPAD (**D**iscriminative **P**erception via **A**nchored **D**escription). DPAD introduces a discriminative signal to operate in synergy with the geometric rewards by compelling the model to generate an anchored and descriptive caption, subsequently quantifying this caption’s discriminative capability through an innovative criterion that contrasts its semantic relevance to the anchored region against its relevance to the wider image context. By optimizing for this discriminative capability, the model’s internal reasoning is implicitly rendered more focused and efficient, leading to an average reduction of approximately 42% in the length of the generated reasoning chains, as shown in Figure 1. Moreover, the caption offers a transparent explanation for the segmentation, improving interpretability. We conduct extensive experiments on benchmark datasets to validate our approach, demonstrating that it delivers substantial performance gains alongside a more focused and efficient reasoning process.

To summarize as follows:

- We introduce Discriminative Perception and propose DPAD, which incentivizes focused reasoning via contrastive discrimination based on an anchored description.
- Extensive experiments on challenging reasoning segmentation benchmarks validate that DPAD achieves substan-

tial performance gains.

- Moreover, DPAD provides interpretability through a co-generated descriptive caption and reduces the average length of reasoning chains by approximately 42%.

2. Related Work

2.1. Image Segmentation

Image segmentation [5, 30], a fundamental task in computer vision, involves partitioning an image into pixel-level masks. The task has evolved from general semantic segmentation to more nuanced, language-driven objectives. A key development in this area is Referring Expression Segmentation [15, 32], which requires segmenting an object specified by a direct natural language phrase and is evaluated on standard benchmarks like RefCOCO, RefCOCO+, and RefCOCOG [34]. Pushing this frontier further, RS [3, 22] challenges models to perform pixel-level localization based on more complex language instructions that require inference. This task demands a deep synthesis of visual perception and language comprehension to decipher relational and abstract cues, thus necessitating models with powerful reasoning abilities.

2.2. Multimodal Large Language Models

The development of MLLMs [13] represents a significant breakthrough in artificial intelligence, bridging the gap between visual perception and natural language understanding. Pre-trained on vast image-text datasets, these models build internal representations that capture a deep semantic alignment between modalities, allowing them to excel at diverse tasks like visual question answering [10], image captioning [16, 31, 35], and complex reasoning [4]. Their ability to comprehend nuanced, context-dependent queries establishes them as a foundational technology for advanced vision-language tasks. These powerful, general-purpose reasoning capabilities, once demonstrated on high-level, holistic image tasks, now pave the way for specialized downstream applications that demand fine-grained, pixel-level understanding, such as reasoning segmentation [22].

2.3. Reasoning Segmentation with MLLMs

Reasoning segmentation leverages the advanced capabilities of MLLMs to perform pixel-level localization based on complex language instructions. The development of this field has undergone a critical paradigm shift from Supervised Fine-Tuning (SFT) to Reinforcement Learning (RL). Early representative methods, such as LISA [11], applied SFT but faced limitations in generalization when dealing with out-of-distribution (OOD) scenarios. To address this issue, the state-of-the-art has shifted towards RL-based methods, represented by Seg-Zero [17]. By employing techniques such as Group-Relative Policy Optimization

(GRPO), these models can elicit the emergent generation of chains of thought without explicit reasoning supervision, significantly enhancing zero-shot performance. Concurrently, this paradigm introduces new considerations for reward mechanism design. The geometric reward signals that current methods rely on provide only localization guidance and are unable to discriminate the quality of the reasoning chain. During the learning process, a model might find a pathway that achieves the final localization, but this pathway is not necessarily the most focused or insightful.

3. Methodology

This section details our proposed method, DPAD. Within an RL-driven framework, DPAD complements rewards for format adherence and geometric accuracy by fostering the model’s “Discriminative Perception” for more focused and efficient reasoning segmentation.

3.1. Problem Formulation

Reasoning segmentation, the task of generating a mask M from a given image I and a language query Q , is formulated in our work within an RL framework built upon a decoupled architecture. In this paradigm, a trainable MLLM acts as a reasoning policy, π , to produce localization prompts. These prompts are then consumed by a frozen segmentation model to render the final mask.

For a given state $s = (I, Q)$, this policy is trained to generate a token sequence Y containing a reasoning chain T , a geometric localization A , and an anchored descriptive caption C , with the generation process expressed as:

$$Y = (T, A, C) \sim \pi(\cdot|s) \quad (1)$$

The final mask M is then deterministically produced by the localization A via a frozen segmentation module, \mathcal{F}_{seg} , such that $M = \mathcal{F}_{seg}(I, A)$. The overarching objective of the RL framework is to learn an optimal policy π^* that maximizes the expected final reward, R_{final} . This reward function directly evaluates the quality of the generated sequence Y . The optimization objective is formally defined as:

$$\pi^* = \arg \max_{\pi} \mathbb{E}_{Y \sim \pi(\cdot|s)} [R_{final}(Y, s)] \quad (2)$$

3.2. Discriminative Perception

To address the unfocused and verbose reasoning chains produced by existing RL frameworks, we introduce DPAD (Discriminative Perception via Anchored Description), as shown in Figure 2. Our method stimulates the model’s “Discriminative Perception” by requiring the MLLM policy to generate an *anchored descriptive caption* for its localization, which in turn enables a discriminative reward. This process compels the generation of more focused and efficient reasoning chains.

Anchored Descriptive Caption. In addition to the reasoning chain (T) and geometric localization (A), our framework requires the MLLM policy to generate a concise and anchored caption (C). This caption’s purpose is twofold. First, it serves as a human-readable rationale that explains the model’s final localization, enhancing the framework’s overall interpretability. Second, and more critically, it acts as the semantic foundation for our reward signal, providing the necessary content to evaluate the model’s discriminative ability. The caption is considered “anchored” because it is prompted to describe the object identified by the model’s own geometric localization output (A).

Discriminative Perception Reward. This reward is the technical core of DPAD, designed to quantify and incentivize the model’s discriminative perception. As illustrated in Figure 2, this reward, R_{dpad} , is calculated by contrasting the caption’s relevance to the target versus the broader context. To achieve this, we define the Region of Interest (ROI) as the image crop bounded by the ground-truth box, and the All of Image (AOI) as the entire image. Using a pre-trained vision-language model (e.g., CLIP), we extract semantic features from both the text and the image modalities. Let V_C denote the text feature embedding of the caption C , and let V_{ROI} and V_{AOI} denote the visual feature embeddings of the ROI and AOI, respectively. The semantic similarity function between a generic text feature vector V_T and a visual feature vector V_I is defined as follows:

$$\text{Sim}(V_T, V_I) = \frac{V_T \cdot V_I}{\|V_T\| \|V_I\|} \quad (3)$$

Based on this, we derive ROI Score, $S_1 = \text{Sim}(V_C, V_{ROI})$, and AOI Score, $S_2 = \text{Sim}(V_C, V_{AOI})$. An effective caption must be more relevant to the ROI than to the image as a whole. We thus formulate our final discriminative signal, Δ , to reflect this principle:

$$\Delta = \max(0, S_1 - S_2) \quad (4)$$

Here, the term $(S_1 - S_2)$ quantifies the discriminative power of the caption. The discriminative reward, R_{dpad} , is then formalized as follows:

$$R_{dpad} = \begin{cases} 1, & \text{if } \Delta > 0 \\ 0, & \text{if } \Delta = 0 \end{cases} \quad (5)$$

3.3. Final Reward and Optimization

The complete reward signal, R_{final} , is a composite function designed to guide the policy from multiple perspectives, as illustrated in Figure 2. It is composed of three components.

Format Validation Reward (R_{format}). This reward ensures the model’s outputs adhere to a predefined structure. We employ three specific checks. First, a regular expression verifies the presence and order of the `<think>`,

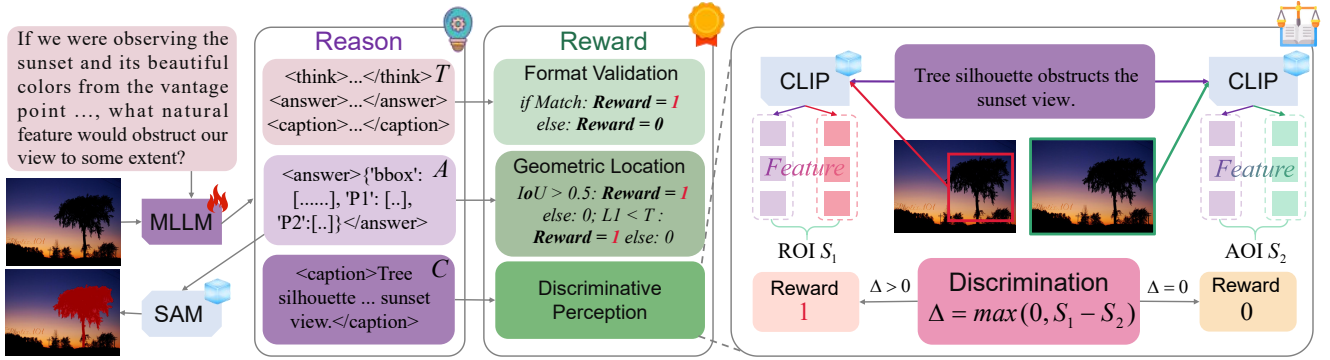


Figure 2. An overview of the DPAD framework, where a MLLM generates a reasoning chain (T), a geometric localization (A), and an anchored descriptive caption (C). The core of our method is the Discriminative Perception reward, which uses the generated caption to derive a Region of Interest (ROI) Score (S_1) and an All of Image (AOI) Score (S_2). The contrast between these scores provides a binary reward signal that incentivizes the model to generate focused reasoning capable of distinguishing the target from its context.

<answer>, and <caption> tags. Second, a parser validates the JSON object within the <answer> tag, ensuring it contains the required keys (“bbox”, “points_1”, “points_2”) and that their values are correctly formatted. Finally, a check confirms the presence of an anchored descriptive caption (C) within the model’s output. All checks return a binary reward of 1.0 for success and 0.0 for failure, ensuring strict adherence to the desired output format.

Geometric Location Reward (R_{geo}). This reward evaluates the geometric accuracy of the localization output (A) to enhance spatial precision. It is a composite of several sub-rewards. An IoU-based reward is calculated, yielding a score of 1.0 if the Intersection over Union between the predicted and ground-truth bounding boxes exceeds 0.5, and 0.0 otherwise. We also employ L_1 distance-based rewards for both the bounding box and key points. These provide a reward of 1.0 if the distance is below a set threshold and 0.0 otherwise. This combination of metrics ensures the localization is both spatially accurate and correctly positioned.

The final reward is formulated as follows:

$$R_{\text{final}} = R_{\text{format}} + R_{\text{geo}} + R_{\text{dpad}} \quad (6)$$

Optimization. The MLLM policy, π , is then fine-tuned using GRPO to maximize the expected R_{final} . By optimizing this composite objective, the policy is compelled to generate reasoning chains that are not only geometrically accurate but also semantically focused. This process implicitly prunes divergent and verbose thoughts, forcing the model to concentrate on the unique attributes that distinguish the target, thereby leading to more efficient reasoning and improved segmentation performance.

Table 1. Performance comparison on existing benchmarks. Symbol † denotes scores reported in the paper while * denotes our reproduction with official code and model checkpoint. Our method achieves improvements on ReasonSeg.

Method	val		test	
	gIoU	cIoU	gIoU	cIoU
OVSeg	28.5	18.6	26.1	20.8
ReLA	22.4	19.9	21.3	22.0
Grounded-SAM	26.0	14.5	21.3	16.4
LISA-7B-LLaVA1.5	53.6	52.3	48.7	48.8
LISA-13B-LLaVA1.5	57.7	60.3	53.8	50.8
SAM4MLLM	46.7	48.1	-	-
Qwen2.5VL-3B + SAM2	53.8	44.1	47.6	37.4
Seg-Zero-7B†	62.6	62.0	57.5	52.0
Seg-Zero-7B*	60.9	57.3	57.7	54.4
DPAD-7B (ours)	63.1	61.2	60.8	57.5

4. Experiments

4.1. Experimental Settings

We adopt a frozen CLIP model (ViT-B/32) as the semantic scorer to extract both textual and visual features for the computation of R_{dpad} . To rigorously evaluate our proposed method, DPAD, we utilize a range of standard benchmarks for reasoning and referring expression segmentation.

Training Data. Our model is trained exclusively on a small subset of 3,000 samples from the RefCOCOg dataset [34]. This minimal training set is smaller than those used in prior works, which underscores the superior data and learning efficiency of our method. We do not use any datasets with explicit reasoning chain annotations for training.

Evaluation Benchmarks. The performance of our proposed method, DPAD, is evaluated on several benchmarks.

Table 2. Performance comparison on existing benchmarks. Symbol † denotes scores reported in the paper while * denotes our reproduction with official code and model checkpoint. Our method achieves improvements in cIoU on RefCOCO, RefCOCO+, and RefCOCOg.

Method	RefCOCO testA	RefCOCO+ testA	RefCOCOg test
LAVT	75.8	68.4	62.1
ReLA	76.5	71.0	66.0
LISA-7B	76.5	67.4	68.5
PixelLM-7B	76.5	71.7	70.5
MagNet	78.3	73.6	69.3
Seg-Zero-7B†	80.3	76.2	72.6
Seg-Zero-7B*	78.7	74.4	71.3
DPAD-7B (ours)	79.3	74.7	72.6

We use ReasonSeg as our primary benchmark to assess the model’s generalization capability on complex and nuanced queries. Furthermore, the model’s robustness and zero-shot transfer capabilities are validated on the standard test splits of RefCOCO, RefCOCO+, and RefCOCOg.

4.2. Evaluation Metrics

We evaluate our model from two perspectives: segmentation performance and discriminative perception capability.

Segmentation Performance. We adopt global Intersection over Union (gIoU) and cumulative Intersection over Union (cIoU) to rigorously assess pixel-level mask prediction. Specifically, gIoU averages the IoU scores across all samples to provide a robust instance-level evaluation that weights small and large targets equally. Conversely, cIoU computes the ratio of total intersection to total union areas across the entire dataset, offering a stable macro-level measurement of pixel precision.

Discriminative Perception Capability. To evaluate the discriminative specificity of the model’s outputs towards the target, we introduce a suite of semantic metrics for both the descriptive caption (C) and the reasoning chain (T). For the caption, we measure its similarity to the ROI (S_1) and the AOI (S_2), deriving a Semantic Signal-to-Noise Ratio ($\text{SNR} = S_1/S_2$) to quantify its discriminative power. Similarly, to analyze the internal reasoning process, we compute TS_1 and TS_2 as the similarities of T to the ROI and AOI, respectively, yielding the Reasoning SNR ($\text{TSNR} = TS_1/TS_2$). High values for S_1 and TS_1 indicate strong target relevance, while high SNR and TSNR demonstrate precise contextual specificity.

4.3. Implementation Details

Architecture. Our framework follows a decoupled design. We use Qwen2.5-VL [2] as the reasoning model and

Table 3. Performance and efficiency across different Query Types on ReasonSeg.

Query	gIoU (↑)		#Tok (↓)	
	Base	DPAD	Base	DPAD
Attribute	61.22	64.29	97.76	59.95
Relation	58.47	62.17	91.73	63.00
Logic	44.92	47.03	110.22	68.30

Table 4. Performance and efficiency across different Difficulty levels on ReasonSeg.

Difficulty	gIoU (↑)		#Tok (↓)	
	Base	DPAD	Base	DPAD
Easy	68.37	73.04	91.62	59.28
Medium	58.91	61.69	96.29	61.66
Hard	45.19	47.48	105.06	62.17

Table 5. Comparison of discriminative perception metrics for DPAD and Seg-Zero on ReasonSeg.

Metric	Seg-zero-7B		DPAD-7B (ours)	
	val	test	val	test
Tokens#	117.50	111.90	68.49	68.52
S_1	-	-	25.54	25.53
S_2	-	-	22.77	22.63
SNR	-	-	1.15	1.16
TS_1	21.83	23.18	22.14	22.07
TS_2	22.37	24.74	21.28	21.31
TSNR	0.98	0.94	1.05	1.04

a frozen SAM2-Large [20] as the segmentation module.

Training. We use a batch size of 16 and a sampling number of 8 for each training step. The initial learning rate is set to 1×10^{-6} with a weight decay of 0.01. The reward weights λ are fixed at 1.0 by default. The discriminative reward R_{dpad} is calculated using a frozen CLIP (ViT-B/32) model, which is entirely discarded during inference.

4.4. Experimental Results

Segmentation Performance. We compare our method, DPAD, against a comprehensive suite of state-of-the-art approaches, including OVSeg [14], ReLA [14], Grounded-SAM [21], LISA-7B-LLaVA1.5 [11], LISA-13B-LLaVA1.5 [11], SAM4MLLM [4], Qwen2.5VL-3B + SAM2 [27], LAVT [32], PixelLM-7B [22], MagNet [6], and Seg-Zero-7B [17]. As demonstrated in Table 1 and Table 2, our DPAD-7B achieves state-of-the-art performance across multiple challenging benchmarks. On the ReasonSeg dataset, DPAD-7B yields substantial improvements over the

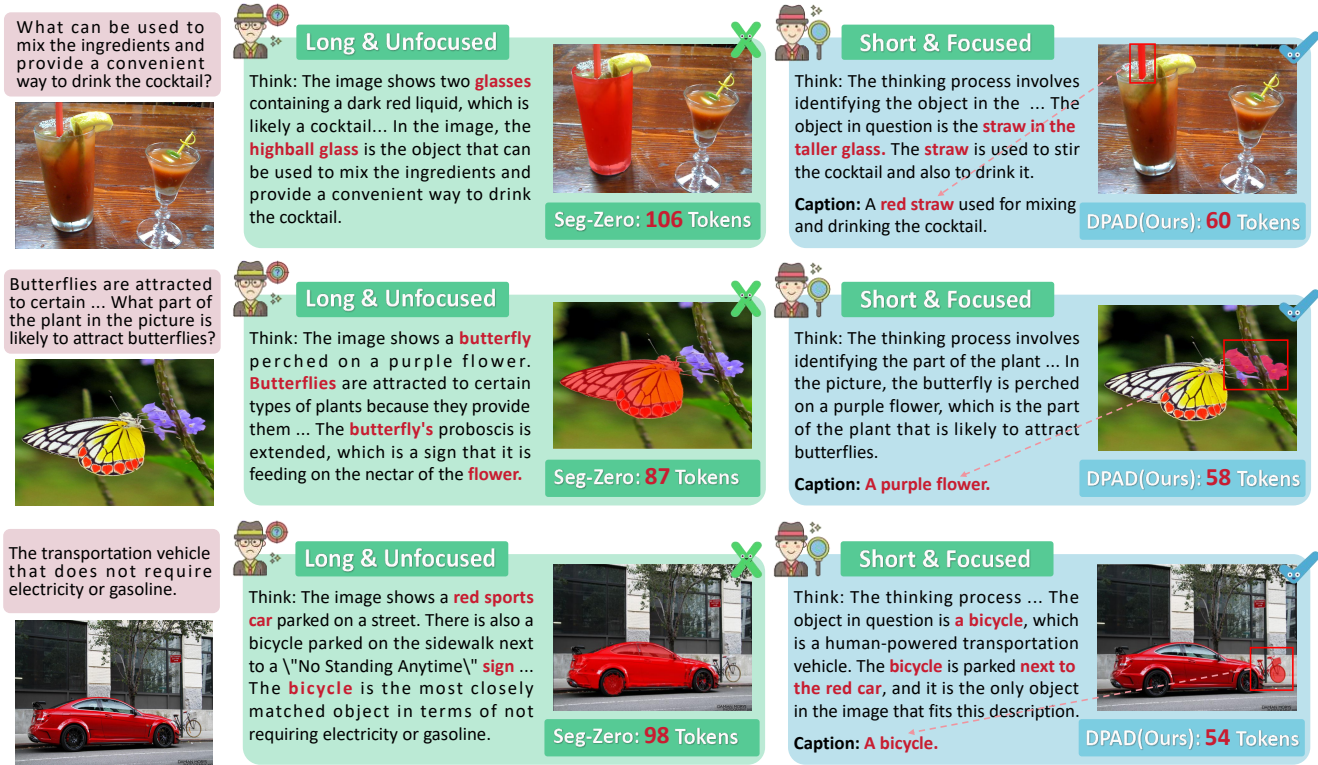


Figure 3. Qualitative comparison between the Seg-Zero and our DPAD. The figure illustrates examples where Seg-Zero produces “Long & Unfocused” reasoning chains that often stray into irrelevant context before identifying the target. In contrast, DPAD generates “Short & Focused” chains that are more converged and efficient. This demonstrates how DPAD’s Discriminative Perception leads to more precise reasoning and a significant reduction in token count.

strong Seg-Zero-7B* baseline, boosting gIoU from 57.7 to 60.8 (+3.1) and cIoU from 54.4 to 57.5 (+3.1). This significant gain confirms that explicitly cultivating discriminative perception enhances the model’s capacity to disambiguate targets from complex distractors. Furthermore, we evaluate the zero-shot generalization of DPAD-7B on the RefCOCO, RefCOCO+, and RefCOCog test splits. As shown in Table 2, our model outpaces the Seg-Zero-7B* across all three datasets, achieving 79.3 (+0.6) on RefCOCO, 74.7 (+0.3) on RefCOCO+, and 72.6 (+1.3) on RefCOCog. These consistent improvements underscore that our discriminative reward mechanism inherently strengthens cross-domain robustness and zero-shot transferability.

Stratified Analysis. To further investigate the robustness of our approach, we stratify the ReasonSeg test set by query type (Attribute, Relation, Logic) and difficulty (Easy, Medium, Hard). Following the complexity assessment protocol in [27], we utilize Qwen2.5-VL-72B to categorize the queries based on scene ambiguity and cognitive complexity. As detailed in Table 3 and Table 4, DPAD consistently outperforms the baseline across all data splits. When examining query types (Table 3), the baseline exhibits a clear token explosion on complex Logic queries, consuming over 110

Table 6. Comparison of discriminative perception metrics for DPAD and Seg-Zero on RefCOCO testA (o), RefCOCO testA (+), RefCOCog test (g).

Metric	Seg-zero-7B			DPAD-7B (ours)		
	o	+	g	o	+	g
Tokens#	165.1	159.9	159.8	63.13	62.88	66.79
S ₁	-	-	-	24.30	24.64	25.91
S ₂	-	-	-	20.54	19.51	22.28
SNR	-	-	-	1.24	1.34	1.21
TS ₁	19.66	19.69	20.15	21.83	21.30	22.67
TS ₂	21.41	21.36	22.50	19.82	18.98	20.98
TSNR	0.92	0.93	0.90	1.11	1.14	1.09

tokens on average. DPAD successfully mitigates this verbosity, compressing the reasoning chain by approximately 38% while still delivering a +2.11 gIoU improvement. Furthermore, DPAD achieves even more pronounced accuracy gains on Attribute (+3.07 gIoU) and Relation (+3.70 gIoU) queries, demonstrating its broad versatility. A similarly compelling trend emerges across varying difficulty levels

Table 7. Ablation of reward formulations on ReasonSeg. The best results are highlighted in bold.

Method	val		test	
	gIoU	cIoU	gIoU	cIoU
Baseline	60.9	57.3	57.7	54.4
+ Difference	61.3	58.8	57.6	54.3
+ Scaled	62.6	54.0	58.4	57.5
DPAD (Binary)	63.1	61.2	60.8	57.5

(Table 4). On Easy and Medium subsets, DPAD secures substantial performance boosts of +4.67 and +2.78 gIoU. Notably, on the most challenging Hard scenarios, DPAD yields a +2.29 improvement in gIoU while drastically reducing the reasoning token count by nearly 41% (from 105.06 to 62.17). Crucially, while the baseline’s token usage fluctuates wildly with task complexity, DPAD maintains a remarkably stable reasoning length ranging only from 59 to 68 tokens across all stratifications. These fine-grained results robustly validate our core premise that pruning divergent thoughts effectively cultivates a generalizable and efficient reasoning paradigm without compromising the model’s capacity for complex logical deduction.

Discriminative Perception Capability. Beyond segmentation accuracy, we analyze the model’s internal behavior using our proposed metrics to strictly assess discriminative capability and reasoning efficiency. As detailed in Table 5 and Table 6, DPAD-7B consistently achieves SNR and TSNR values exceeding the critical threshold of 1.0 across all test sets, whereas the Seg-Zero-7B baseline consistently falls below this mark. On the ReasonSeg benchmark, for instance, DPAD-7B records an SNR of 1.16 and a TSNR of 1.04. Surpassing this 1.0 threshold signifies that the generated text aligns more closely with the target ROI than with the broader image context. This provides direct quantitative evidence that DPAD acquires true discriminative perception, effectively distinguishing the target from background distractors and mitigating the tendency of prior methods to incorporate irrelevant contextual noise. Furthermore, this enhanced target focus directly translates to vastly improved reasoning efficiency. Evaluated by the average token count, DPAD-7B generates significantly more concise reasoning chains. On the ReasonSeg test set, the required token count drops from 117.90 to 68.52 (a 41.7% reduction). A similar trend emerges across the RefCOCO variants, with the RefCOCOg test set exhibiting a substantial decrease from 159.80 to 66.79 (a 58.2% reduction). These compelling results lend robust empirical support to our hypothesis that optimizing for discriminative perception implicitly prunes divergent thoughts, thereby compelling the model toward highly converged and efficient reasoning.

Qualitative Analysis. To provide an intuitive under-

Table 8. Ablation study of different reward formulations in cIoU on RefCOCO, RefCOCO+, and RefCOCOg test sets, showing cIoU scores. Best results are highlighted in bold.

Method	RefCOCO	RefCOCO+	RefCOCOg
	testA	testA	test
Baseline	78.7	74.4	71.3
+ Difference	77.2	73.2	70.8
+ Scaled	78.4	74.6	71.6
DPAD (Binary)	79.3	74.7	72.6

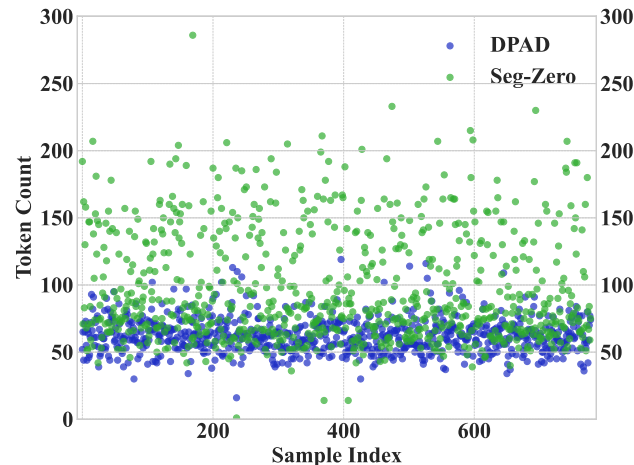


Figure 4. Per-sample token count comparison on the ReasonSeg test. DPAD is shown in blue, and Seg-Zero is shown in green.

standing of our method’s impact, we present a multi-faceted analysis in Figure 3, Figure 4, and Figure 5.

Figure 3 presents a direct qualitative comparison between the reasoning processes of DPAD and the Seg-Zero baseline. The visualizations illustrate how DPAD’s core principle, Discriminative Perception, addresses the verbose and unfocused chains typical of prior methods. By explicitly incentivizing target-relevant descriptions, our framework actively prunes divergent global scenes, irrelevant objects, and redundant self-confirmations from the internal thought process. For instance, in identifying an object for a cocktail, Seg-Zero strays into irrelevant context, while DPAD immediately identifies the correct object (the straw), effectively cutting the token count from 106 to 60. This powerful disambiguation capability is equally evident in the non-electric vehicle example; DPAD avoids distraction from the visually dominant sports car and correctly locates the bicycle, reducing the token count from 98 to 54.

This efficiency is not an anomaly. Figure 4 extends this analysis to every sample in the ReasonSeg test set, plotting the token count for each individual inference. The scatter plot reveals that DPAD’s token counts (blue) are consis-

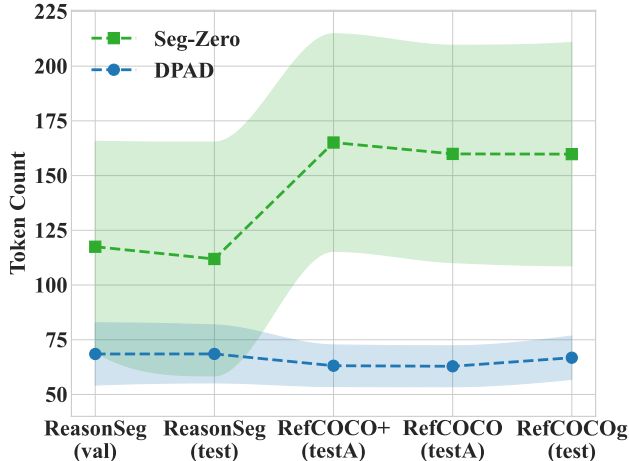


Figure 5. Comparison of the average token counts generated by DPAD and Seg-Zero across five datasets. The lines represent the mean values, while the shaded areas indicate the standard deviation. The results confirm that DPAD accomplishes accurate reasoning using significantly fewer tokens and exhibiting lower variance across all benchmarks.

tently clustered in a low, tight band, demonstrating stable and highly efficient performance. In contrast, Seg-Zero’s counts (green) are not only significantly higher on average but also exhibit much greater variance across samples.

Furthermore, Figure 5 provides compelling evidence for how our method’s focused reasoning translates into superior efficiency and stability across five distinct benchmarks. As a direct result of our discriminative optimization, DPAD maintains a consistently low average token count (the blue line, approximately 65 tokens) with a narrow variance band, signifying robust, low-variance reasoning. Conversely, Seg-Zero’s unfocused process leads to a substantially higher and more volatile token count. This instability is visually evident in its fluctuating average and wide variance band, revealing a high-variance reasoning process that is overly sensitive to dataset-specific complexities.

Overall, these visualizations robustly support our central thesis that by compelling the model to generate an anchored description and optimizing for a discriminative reward, DPAD successfully cultivates a highly focused and efficient reasoning paradigm. This not only improves quantitative performance but also produces transparent reasoning chains devoid of irrelevant contextual noise.

4.5. Ablation Study

To investigate the impact of different reward formulations, we conduct an ablation study with results detailed in Table 7 and Table 8. We compare our final DPAD model equipped with a binary reward against a Baseline trained without any discriminative signal, alongside two alternative continuous

reward designs. The first alternative is a “Difference” reward formulated as $R = S_1 - S_2$, and the second is a “Scaled” reward calculated as $R = S_1 \times \max(0, S_1 - S_2)$.

A clear performance hierarchy emerges across all benchmarks. On the ReasonSeg dataset (Table 7), all three reward formulations yield improvements over the Baseline. The “Difference” reward improves the validation gIoU to 61.3 (+0.4), while the “Scaled” variant reaches 62.6 (+1.7). Crucially, our binary reward establishes the best performance among all variants, boosting validation gIoU to 63.1 (+2.2) and cIoU to 61.2 (+3.9). This trajectory extends to the RefCOCO experiments (Table 8). All variants surpass the Baseline, with the binary reward uniformly securing the highest scores across the three test splits, highlighted by a notable cIoU of 72.6 on the challenging RefCOCOg benchmark.

We attribute the clear superiority of the binary reward to its signal format, which is highly compatible with the internal optimization mechanics of our framework. Specifically, our system—including the Format Validation reward (R_{format}) and the Geometric Location reward (R_{geo})—fundamentally relies on discrete success-or-failure signals to guide the GRPO-based policy updates. Our binary discriminative reward aligns with this effective paradigm, providing unambiguous feedback on whether the model distinguishes the target. In contrast, while continuous rewards offer more granular semantic information, their inherent numerical noise and scale fluctuations actively interfere with the stable convergence of the RL policy.

5. Conclusion

In this work, we introduced DPAD, a framework that mitigates unfocused reasoning in segmentation models by fostering discriminative perception. By compelling the MLLM to generate an anchored descriptive caption, DPAD learns to explicitly distinguish targets from their context, yielding a highly converged and efficient reasoning process. Extensive experiments demonstrate that DPAD achieves state-of-the-art performance across multiple challenging benchmarks, including ReasonSeg and the RefCOCO suite. Crucially, these accuracy gains are accompanied by an approximate 42% reduction in reasoning chain length and discriminative signals (SNR and TSNR) consistently exceeding the critical 1.0 threshold. Beyond quantitative improvements, DPAD significantly enhances interpretability through its co-generated captions. Ultimately, our findings suggest that optimizing for discriminative perception offers a highly promising pathway toward building accurate, focused, and efficient Multimodal Large Language Models for complex visual reasoning tasks.

Acknowledgments

This work was supported by the National Natural Science Foundation of China under Grants 62471394 and U21B2041.

References

- [1] Pranjal Aggarwal and Sean Welleck. L1: Controlling How Long a Reasoning Model Thinks with Reinforcement Learning. *arXiv preprint arXiv:2503.04697*, 2025. 2
- [2] Shuai Bai, Keqin Chen, Xuejing Liu, Jialin Wang, Wenbin Ge, Sibao Song, Kai Dang, Peng Wang, Shijie Wang, Jun Tang, et al. Qwen2. 5-vl technical report. *arXiv preprint arXiv:2502.13923*, 2025. 5
- [3] Chao Chen, Jiacheng Xu, Weijian Liao, Hao Ding, Zongzhang Zhang, Yang Yu, and Rui Zhao. Focus-then-Decide: Segmentation-assisted Reinforcement Learning. In *Proceedings of the AAAI Conference on Artificial Intelligence*, pages 11240–11248, 2024. 1, 2
- [4] Yi-Chia Chen, Wei-Hua Li, Cheng Sun, Yu-Chiang Frank Wang, and Chu-Song Chen. SAM4MLLM: Enhance Multimodal Large Language Model for Referring Expression Segmentation. In *European Conference on Computer Vision*, pages 323–340. Springer, 2024. 2, 5
- [5] Bowen Cheng, Ishan Misra, Alexander G Schwing, Alexander Kirillov, and Rohit Girdhar. Masked-attention Mask Transformer for Universal Image Segmentation. In *Proceedings of the IEEE/CVF Conference on Computer Vision and Pattern Recognition*, pages 1290–1299, 2022. 2
- [6] Yong Xien Chng, Henry Zheng, Yizeng Han, Xuchong Qiu, and Gao Huang. Mask grounding for referring image segmentation. In *Proceedings of the IEEE/CVF Conference on Computer Vision and Pattern Recognition*, pages 26573–26583, 2024. 5
- [7] Daya Guo, Dejian Yang, Haowei Zhang, Junxiao Song, Ruoyu Zhang, Runxin Xu, Qihao Zhu, Shirong Ma, Peiyi Wang, Xiao Bi, et al. Deepseek-RL: Incentivizing Reasoning Capability in LLMs via Reinforcement Learning. *arXiv preprint arXiv:2501.12948*, 2025. 1
- [8] Duojun Huang, Xinyu Xiong, Jie Ma, Jichang Li, Zequn Jie, Lin Ma, and Guanbin Li. AlignSAM: Aligning Segment Anything Model to Open Context via Reinforcement Learning. In *Proceedings of the IEEE/CVF Conference on Computer Vision and Pattern Recognition*, pages 3205–3215, 2024. 1
- [9] Jiaqi Huang, Zunnan Xu, Jun Zhou, Ting Liu, Yicheng Xiao, Mingwen Ou, Bowen Ji, Xiu Li, and Kehong Yuan. SAM-RL: Leveraging SAM for Reward Feedback in Multimodal Segmentation via Reinforcement Learning. *arXiv preprint arXiv:2505.22596*, 2025. 2
- [10] Ngoc Dung Huynh, Mohamed Reda Bouadjenek, Sunil Aryal, Imran Razzak, and Hakim Hacid. Visual Question Answering: From Early Developments to Recent Advances—A Survey. *arXiv preprint arXiv:2501.03939*, 2025. 2
- [11] Xin Lai, Zhuotao Tian, Yukang Chen, Yanwei Li, Yuhui Yuan, Shu Liu, and Jiaya Jia. Lisa: Reasoning Segmentation via Large Language Model. In *Proceedings of the IEEE/CVF Conference on Computer Vision and Pattern Recognition*, pages 9579–9589, 2024. 1, 2, 5
- [12] Liulei Li, Wenguan Wang, and Yi Yang. LogicSeg: Parsing Visual Semantics with Neural Logic Learning and Reasoning. In *Proceedings of the IEEE/CVF International Conference on Computer Vision*, pages 4122–4133, 2023. 1
- [13] Yanwei Li, Yuechen Zhang, Chengyao Wang, Zhisheng Zhong, Yixin Chen, Ruihang Chu, Shaoteng Liu, and Jiaya Jia. Mini-Gemini: Mining the Potential of Multi-modality Vision Language Models. *arXiv preprint arXiv:2403.18814*, 2024. 2
- [14] Feng Liang, Bichen Wu, Xiaoliang Dai, Kunpeng Li, Yanan Zhao, Hang Zhang, Peizhao Zhang, Peter Vajda, and Diana Marculescu. Open-vocabulary semantic segmentation with mask-adapted clip. In *Proceedings of the IEEE/CVF conference on computer vision and pattern recognition*, pages 7061–7070, 2023. 5
- [15] Chang Liu, Henghui Ding, and Xudong Jiang. Gres: Generalized referring expression segmentation. In *Proceedings of the IEEE/CVF conference on computer vision and pattern recognition*, pages 23592–23601, 2023. 2
- [16] Haotian Liu, Chunyuan Li, Qingyang Wu, and Yong Jae Lee. Visual Instruction Tuning. *Advances in Neural Information Processing Systems*, 36:34892–34916, 2023. 2
- [17] Yuqi Liu, Bohao Peng, Zhisheng Zhong, Zihao Yue, Fanbin Lu, Bei Yu, and Jiaya Jia. Seg-zero: Reasoning-chain Guided Segmentation via Cognitive Reinforcement. *arXiv preprint arXiv:2503.06520*, 2025. 1, 2, 5
- [18] Yuqi Liu, Tianyuan Qu, Zhisheng Zhong, Bohao Peng, Shu Liu, Bei Yu, and Jiaya Jia. VisionReasoner: Unified Visual Perception and Reasoning via Reinforcement Learning. *arXiv preprint arXiv:2505.12081*, 2025. 1
- [19] Xiaoye Qu, Yafu Li, Zhaochen Su, Weigao Sun, Jianhao Yan, Dongrui Liu, Ganqu Cui, Daizong Liu, Shuxian Liang, Junxian He, et al. A Survey of Efficient Reasoning for Large Reasoning Models: Language, Multimodality, and Beyond. *arXiv preprint arXiv:2503.21614*, 2025. 2
- [20] Nikhila Ravi, Valentin Gabeur, Yuan-Ting Hu, Ronghang Hu, Chaitanya Ryali, Tengyu Ma, Haitham Khedr, Roman Rädle, Chloe Rolland, Laura Gustafson, et al. Sam 2: Segment anything in images and videos. *arXiv preprint arXiv:2408.00714*, 2024. 5
- [21] Tianhe Ren, Shilong Liu, Ailing Zeng, Jing Lin, Kunchang Li, He Cao, Jiayu Chen, Xinyu Huang, Yukang Chen, Feng Yan, et al. Grounded SAM: Assembling Open-World Models for Diverse Visual Tasks. *arXiv preprint arXiv:2401.14159*, 2024. 5
- [22] Zhongwei Ren, Zhicheng Huang, Yunchao Wei, Yao Zhao, Dongmei Fu, Jiashi Feng, and Xiaojie Jin. PixelLM: Pixel Reasoning with Large Multimodal Model. In *Proceedings of the IEEE/CVF Conference on Computer Vision and Pattern Recognition*, pages 26374–26383, 2024. 2, 5
- [23] Yiqing Shen, Chenjia Li, Fei Xiong, Jeong-O Jeong, Tianpeng Wang, Michael Latman, and Mathias Unberath. Reasoning Segmentation for Images and Videos: A Survey. *arXiv preprint arXiv:2505.18816*, 2025. 1, 2
- [24] Yang Sui, Yu-Neng Chuang, Guanchu Wang, Jiamu Zhang, Tianyi Zhang, Jiayi Yuan, Hongyi Liu, Andrew Wen,

- Shaochen Zhong, Hanjie Chen, et al. Stop Overthinking: A Survey on Efficient Reasoning for Large Language Models. *arXiv preprint arXiv:2503.16419*, 2025. 2
- [25] Xie Ting, Ye Huang, Zhilin Liu, and Lixin Duan. Semantic Segmentation with Reward. *arXiv preprint arXiv:2505.17905*, 2025. 1
- [26] Junchi Wang and Lei Ke. LLM-Seg: Bridging Image Segmentation and Large Language Model Reasoning. In *Proceedings of the IEEE/CVF Conference on Computer Vision and Pattern Recognition*, pages 1765–1774, 2024. 1
- [27] Song Wang et al. PixelThink: Towards Efficient Chain-of-Pixel Reasoning. *arXiv preprint arXiv:2505.23727*, 2025. 1, 2, 5, 6
- [28] XuDong Wang, Shaolun Zhang, Shufan Li, Konstantinos Kallidromitis, Kehan Li, Yusuke Kato, Kazuki Kozuka, and Trevor Darrell. SegLLM: Multi-round Reasoning Segmentation. *arXiv preprint arXiv:2410.18923*, 2024. 1
- [29] Yibin Wang, Zhimin Li, Yuhang Zang, Chunyu Wang, Qinglin Lu, Cheng Jin, and Jiaqi Wang. Unified Multi-modal Chain-of-Thought Reward Model through Reinforcement Fine-tuning. *arXiv preprint arXiv:2505.03318*, 2025. 2
- [30] Yuwen Xiong, Renjie Liao, Hengshuang Zhao, Rui Hu, Min Bai, Ersin Yumer, and Raquel Urtasun. UPSNet: A Unified Panoptic Segmentation Network. In *Proceedings of the IEEE/CVF Conference on Computer Vision and Pattern Recognition*, pages 8818–8826, 2019. 2
- [31] Tao Yang, Qing Zhou, and Qi Wang. Dia: Deriving linguistic information from auxiliary languages for remote sensing image captioning. *Pattern Recognition*, 171:112209, 2026. 2
- [32] Zhao Yang, Jiaqi Wang, Yansong Tang, Kai Chen, Hengshuang Zhao, and Philip HS Torr. LAVT: Language-aware Vision Transformer for Referring Image Segmentation. In *Proceedings of the IEEE/CVF Conference on Computer Vision and Pattern Recognition*, pages 18155–18165, 2022. 2, 5
- [33] Zuyao You and Zuxuan Wu. Seg-r1: Segmentation can be surprisingly simple with reinforcement learning. *arXiv preprint arXiv:2506.22624*, 2025. 1
- [34] Licheng Yu, Patrick Poirson, Shan Yang, Alexander C Berg, and Tamara L Berg. Modeling Context in Referring Expressions. In *European Conference on Computer Vision*, pages 69–85. Springer, 2016. 2, 4
- [35] Qing Zhou, Junyu Gao, Yuan Yuan, and Qi Wang. Single-stream extractor network with contrastive pre-training for remote-sensing change captioning. *IEEE Transactions on Geoscience and Remote Sensing*, 62:1–14, 2024. 2

Discriminative Perception via Anchored Description for Reasoning Segmentation

Supplementary Material

Query: When taking a dog for a walk on the beach, what part of the dog's body should be wet if it enjoys playing in the water?



Mask IoU=0.19 Baseline: 146 Tokens



Think: The image shows a dog on a beach with its paws in the water. The dog appears to be enjoying itself. The question asks what part of the dog's body should be wet if it enjoys playing in the water. Given the context, the paws of the dog are the part that would be most likely to be wet, as they are in direct contact with the water. The dog's paws are the part of the body that would be wet if it enjoys playing in the water. The paws are the only part of the dog's body that are in the water, and they are the part that would get wet from playing in the water. The answer should be the paws of the dog, as they are the part of the body that would be wet if the dog enjoys playing in the water.



Mask IoU=0.61 DPAD(Ours): 56 Tokens



Think: The thinking process involves identifying the part of the dog's body that would be wet if it enjoys playing in the water. The dog in the image is standing in shallow water, and the part of the dog's body that would be wet is the lower legs and paws.



Caption: The lower legs and paws of the dog.

Query: When a cat is interested in something and wants to observe it carefully, what part of the cat's body in the picture is most likely to be the focus of attention?



Mask IoU=0.25 Baseline: 160 Tokens



Think: The image shows a cat lying on a wooden floor. The cat's body is relaxed, and it is looking directly at the camera with a focused expression. The cat's ears are perked up, which is a common sign of interest. The eyes are wide open, and the pupils are dilated, indicating that the cat is paying close attention to something. In the context of the question, when a cat is interested in something and wants to observe it carefully, the most likely part of the cat's body to be the focus of attention would be the eyes. The eyes are the most expressive part of the cat's face and are the first thing that catches attention when a cat is observing something. In the image, the cat's eyes are clearly visible and appear to be focused on something in front of it. Therefore, the eyes are the most likely part of the cat's body to be the focus of attention.



Mask IoU=0.78 DPAD(Ours): 85 Tokens



Think: The thinking process involves identifying the part of the cat's body that is most likely to be the focus of attention when the cat is interested in something. Typically, when a cat is interested, it will look directly at the object of interest. In the picture, the cat is looking directly at the camera, which suggests it is focused on something in front of it. The part of the body that is most likely to be the focus of attention is the eyes. Caption: The cat's eyes.



Query: The spare tire that is not used currently.



Mask IoU=0.00 Baseline: 135 Tokens



Think: The image shows a vintage race car on display with a spare tire mounted on the side. The car is parked on a grassy area, and there are people in the background observing it. The spare tire is located on the side of the car, and it is clearly visible in the image. The question asks to find the spare tire that is not used currently and compare the difference between objects. The spare tire is the object in question, and it is not currently in use. The difference between the spare tire and the car is that the spare tire is not part of the car's main structure and is not in contact with the ground, while the car is a functional vehicle with a complete structure and is in contact with the ground.



Mask IoU=0.90 DPAD(Ours): 57 Tokens



Think: The thinking process involves identifying the spare tire that is not currently in use. The spare tire is located at the rear of the vehicle, and in this image, it is visible on the right side of the car. The tire is not inflated and is covered with a protective cover, indicating it is not in use.



Caption: The spare tire that is not used currently.

Query: Girl on left no sleeves.



Mask IoU=0.00 Baseline: 133 Tokens



Think: The image shows a group of people sitting on the grass, with some wearing distinctive clothing and accessories. The person in the foreground, wearing a black tank top with text on the back, appears to be the "girl on left no sleeves". The tank top has a visible text that reads "WIR KÖNNEN UNS NICHT EINRICHTEN DEN WIR SIND IM TEIL VON SUCH!". The task is to find the difference between objects and compare the most closely matched one. The objects in the image are the people, and the most closely matched object in this context is the person wearing the black tank top with the text. The answer should be in JSON format, with the bbox of the person and the points of the two largest inscribed circles inside the interested object.



Mask IoU=0.78 DPAD(Ours): 53 Tokens

Think: The thinking process involves identifying the object of interest, which is 'girl on left no sleeves'. The object is the person on the left side of the image, wearing a sleeveless denim vest and a necklace. The focus is on the person's upper body and the sleeveless vest.



Caption: The girl on left no sleeves.

Query: In a baseball game, the pitcher throws the ball to the batter, who tries to hit it. what equipment does the batter use to hit the ball?



Mask IoU=0.00 Baseline: 83 Tokens



Think: The image shows a baseball game with a batter, a catcher, and an umpire. The batter is holding a baseball bat, which is the equipment used to hit the ball. The thinking process involves identifying the object that the batter uses to hit the ball, which is the baseball bat. The objects in the image are the batter, the baseball bat, the catcher, the umpire, and the baseball field. The baseball bat is the object that the batter uses to hit the ball.



Mask IoU=0.90 DPAD(Ours): 41 Tokens

Think: The thinking process involves identifying the object the batter uses to hit the ball. The object in question is the bat, which the batter holds and swings to hit the ball. The bat is the primary equipment used by the batter.



Caption: The bat used by the batter to hit the ball.

Query: Girl kicking.



Mask IoU=0.00 Baseline: 128 Tokens



Think: The image shows a group of children playing soccer on a grassy field. The focus is on a girl in a blue jersey who appears to be kicking a soccer ball. The other children are running, and there are adults in the background. The girl in the blue jersey is the one kicking the ball, and the other children are running towards the ball. The objects in the image include the soccer ball, the children's soccer uniforms, the grassy field, and the adults in the background. The girl in the blue jersey is the one kicking the ball, and the other children are running towards the ball. The most closely matched object is the girl in the blue jersey, as she is the one actively kicking the ball.



Mask IoU=0.96 DPAD(Ours): 55 Tokens

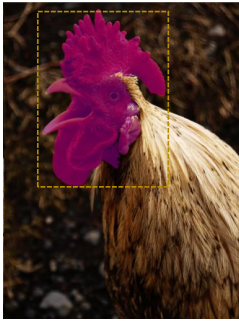
Think: The thinking process involves identifying the object of interest, which is the girl kicking the soccer ball. I look for the person who is actively kicking the ball, which is the girl in the white jersey. The other players and the coach are not the focus.



Caption: The girl in the white jersey kicking the soccer ball.

Figure 6. Additional qualitative comparison. Masks: GT (green), DPAD (red), and baseline (purple).

Query: In the picture, there is a type of bird with a distinctive feature on the top of its head, which usually indicates its gender, what part in the picture might have this characteristic?



<think>The image shows a close-up of a rooster, which is a type of bird. The distinctive feature on the top of its head is the comb, which is a red, fleshy structure. This comb is a characteristic feature of roosters and is used to indicate their gender. The rooster in the image has a red comb. The comb is located on the top of the rooster's head, above the beak and eyes. The rooster's comb is the part of the bird that has the distinctive feature, which is the red fleshy structure on the top of its head.

</think><answer>{"bbox": [204, 21, 786, 258], "points_1": [289, 159], "points_2": [642, 225]}</answer><caption>the rooster's red head </caption> IoU=0.40

Think Format=1 Seg Format=1 IoU=0 Bbox=0 Points=1 DPAD=0 Final=3



<think> The thinking process involves identifying the distinctive feature on the top of the bird's head, which is typically a comb and wattle in roosters. The comb is the red, fleshy structure on top of the bird's head, and the wattle is the hanging flap of skin below the beak. In the picture, the red, fleshy structure on top of the bird's head is the comb. </think><answer>{"bbox": [202, 19, 572, 250], "points_1": [330, 130], "points_2": [420, 200]}</answer><caption>the red comb on the top of the rooster's head</caption> IoU=0.96

</think><answer>{"bbox": [202, 19, 572, 250], "points_1": [330, 130], "points_2": [420, 200]}</answer><caption>the red comb on the top of the rooster's head</caption> IoU=0.96

Think Format=1 Seg Format=1 IoU=1 Bbox=1 Points=1 DPAD=1 Final=6

Figure 7. Qualitative demonstration of spatial-semantic alignment evolution via discriminative perception.

6. Additional Qualitative Analysis

It can be observed that models lacking the “Discriminative Perception” reward often generate verbose and divergent reasoning chains, as detailed in Figure 6. Specifically, DPAD significantly reduces reasoning redundancy across the following three core dimensions:

Pruning Divergent Global Scenes. In the baseline method, the model frequently allocates excessive attention to global background descriptions irrelevant to the query. For instance, in the “spare tire” and “girl kicking” examples, the baseline model consumes a large number of tokens describing the “vintage race car... parked on a grassy area,” “people in the background,” or “adults in the background”. In contrast, DPAD, through the contrastive reward mechanism of anchored descriptions, effectively guides the model to disregard these divergent global details and anchor its reasoning directly on the target object (e.g., clearly locating the uninflated spare tire on the side of the car). This achieves accurate segmentation using significantly fewer tokens (e.g., reducing the count from 135 to 57).

Filtering Irrelevant Objects and Over-identification. When multiple objects or complex semantics are present in a scene, the baseline model is highly prone to enumerative behavior or deviating from the core task. In the “baseball game” example, the baseline not only describes the batter

but also redundantly lists the catcher, the umpire, and the baseball field. This is particularly evident in the “girl on left no sleeves” example, where the baseline diverges from the visual grounding objective to recognize and transcribe a large block of German text (“WIR KÖNNEN UNS NICHT EINRICHTEN...”) on the person’s clothing. DPAD effectively filters out these distractors and precisely converges on the “bat” and the “sleeveless denim vest,” which not only reduces the token count by more than half but also substantially improves the mask IoU from 0.00 to high-precision levels (0.90 and 0.78, respectively).

Reducing Over-reasoning and Self-confirmations. In the examples of the “dog’s paws” and “cat’s eyes,” the baseline exhibits a pronounced tendency toward “self-confirmation.” The model repeatedly restates the problem context and incorporates superfluous trivial details (such as repeatedly emphasizing that the cat’s “ears are perked up” and “pupils are dilated,” or that the dog “appears to be enjoying itself”). DPAD, on the other hand, presents a highly “Short & Focused” reasoning paradigm, addressing the core attributes of the target directly and concisely outputting the “lower legs and paws” or the “cat’s eyes.”

These additional visualization results provide compelling evidence that, by incentivizing target-relevant descriptions, DPAD structurally prunes divergent scenes, irrelevant objects, and uninformative self-confirmations. This

not only substantially compresses the length of the reasoning chains (mitigating the redundancy issues that degrade reasoning efficiency) but, more importantly, provides highly precise localization cues for downstream mask generation by eliminating contextual noise.

7. Evolution of DPAD Alignment

In the evolution analysis of the convergence process, we observe how the DPAD reward mechanism calibrates spatial outputs through differentiated feedback on intermediate states (as shown in Figure 7). During the under-converged stages of training, the model frequently exhibits a disconnect between semantics and geometry. At this stage, if the model relies solely on visual priors to yield a coarse bounding box covering most of the rooster’s head, but generates an over-generalized or inaccurate description (e.g., “the rooster’s red head”), our mechanism assigns a reward of $R = 0$ to suppress such blind localization lacking rigorous logical support. When the model demonstrates correct anatomical discrimination during its reasoning process (e.g., explicitly distinguishing between the “comb on top of the head” and the “wattle under the beak”) and generates the precise description “the red comb on the top of the rooster’s head”, the mechanism provides positive feedback of $R = 1$. Continuously driven by this mechanism, the model is able to correct the initially ambiguous boundaries, precisely contracting and locking the bounding box onto the comb region, raising the IoU to 0.96.